Journal of Autoimmunity 147 (2024) 103255

Contents lists available at ScienceDirect

Journal of Autoimmunity

journal homepage: www.elsevier.com/locate/jautimm

Circulating extracellular vesicles and small non-coding RNAs cargo in idiopathic inflammatory myopathies reveal differences across myositis subsets

Chiara Franco [a,#], Alessandra Giannella [b,#], Michela Gasparotto [a], Elisabetta Zanatta [a], Anna Ghirardello [a], Federico Pettorossi [a], Zahrà Rahmè [a], Roberto Depascale [a], Davide Ragno [a], Gioele Bevilacqua [c], Elisa Bellis [d], Luca Iaccarino [a], Andrea Doria [a,*], Giulio Ceolotto [c,1], Mariele Gatto [a,d,1]

[a] Unit of Rheumatology, Department of Medicine, University of Padua, Padua, Italy
[b] Division of Thrombotic and Hemorrhagic Diseases, Department of Medicine, University of Padua, Padua, Italy
[c] Unit of Emergency Medicine, Department of Medicine, University of Padua, Padua, Italy
[d] Academic Rheumatology Centre, Department of Clinical and Biological Sciences, University of Turin, AO Mauriziano, Turin, Italy

ARTICLE INFO

Keywords:
Idiopathic inflammatory myopathies
Extracellular vesicles
microRNAs
Biomarkers

ABSTRACT

Objective: To investigate the epigenetic footprint of idiopathic inflammatory myopathies (IIM) through characterization of circulating extracellular vesicles (EVs) and the expression of EV-derived small non-coding RNAs (sncRNAs).

Methods: In this cross-sectional study, EVs were isolated by size-exclusion chromatography from plasma of patients with IIM and age- and sex-matched healthy donors (HD). EV-derived sncRNAs were sequenced and quantified using Next-Generation Sequencing (NGS). Following quality control and normalization, filtered count reads were used for differential microRNA (miRNA) and piwi-interacting RNA (piRNA) expression analyses. Putative gene targets enriched for pathways implicated in IIM were analyzed. Patients' clinical and laboratory characteristics at the time of sampling were recorded.

Results: Forty-seven IIM patients and 45 HD were enrolled. MiR-486-5p ($p < 0.01$), miR-122-5p, miR-192-5p, and miR-32-5p were significantly upregulated ($p < 0.05$ for all), while miR-142-3p ($p < 0.001$), miR-141-3p ($p < 0.01$), let-7a-5p ($p < 0.05$) and miR-3613-5p ($p < 0.05$) downregulated in EVs from IIM patients versus HD. MiR-486-5p was associated with raised muscle enzymes levels. Several target genes of up/downregulated miRNAs in IIM participate in inflammation, necroptosis, interferon and immune signaling. Six piRNAs were significantly dysregulated in IIM EVs versus HD ($p < 0.05$). Within IIM, miR-335-5p was selectively upregulated and miR-27a-5p downregulated in dermatomyositis ($n = 21$, $p < 0.01$). Finally, plasma EV levels were significantly increased in cancer-associated myositis (CAM, $n = 12$) versus non-CAM IIM ($n = 35$, $p = 0.02$) and HD ($p < 0.01$). EVs cargo in CAM was significantly enriched of let-7f-5p and depleted of miR-143-3p.

Conclusion: Through an unbiased screening of EV-derived sncRNAs, we characterize miRNAs and piRNAs in the EVs cargo as potential biomarkers and modifiers of diverse IIM phenotypes.

* Corresponding author.
E-mail addresses: chiara.franco@aopd.veneto.it (C. Franco), alessandra.giannella@unipd.it (A. Giannella), gasparotto.michela@gmail.com (M. Gasparotto), elisabetta.zanatta@unipd.it (E. Zanatta), anna.ghirardello@unipd.it (A. Ghirardello), fedepetto@gmail.com (F. Pettorossi), zahra.rahme@studenti.unipd.it (Z. Rahmè), rob.depascale93@gmail.com (R. Depascale), davide.ragno@studenti.unipd.it (D. Ragno), gioele.bevilacqua@studenti.unipd.it (G. Bevilacqua), elisa.bellis@unito.it (E. Bellis), luca.iaccarino@unipd.it (L. Iaccarino), adoria@unipd.it (A. Doria), giulio.ceolotto@unipd.it (G. Ceolotto), mariele.gatto@unito.it (M. Gatto).
[#] Contributed equally and share first-authorship.
[1] Contributed equally and share last-authorship.

https://doi.org/10.1016/j.jaut.2024.103255
Received 16 February 2024; Received in revised form 4 May 2024; Accepted 8 May 2024
Available online 25 May 2024

1. Introduction

Idiopathic inflammatory myopathies (IIM) are a group of rare heterogeneous immune-mediated disorders with a wide spectrum of muscular and extra-muscular involvement [1], encompassing different clinically defined subsets [2]. Among those, dermatomyositis (DM), anti-synthtease syndrome (ASyS) and polymyositis (PM) are the best characterized primitive forms [2]. Besides, cancer-associated myositis (CAM) represents a distinguished subset signifying a paramalignant phenomenon with a unique pathogenesis [3]. In fact, malignancies typically occur within 3 years before or after the onset of myositis, with the overall risk peaking within 1 year of IIM diagnosis, submitting CAM as a consequence of an immune response elicited by the presence of a rising cancer [3].

IIM pathogenesis is characterized by inflammatory mechanisms, innate and adaptive immune abnormalities and non-immune mechanisms stemming on a genetically predisposing background upon environmental triggers [4]. Serologic markers of IIM include myositis-specific antibodies (MSAs), e.g. anti-MDA5, anti-TIF1-γ, anti-Mi2 and anti-tRNA synthetase, and myositis-associated antibodies (MAAs) shared across other rheumatic diseases, including anti-Ro/SSA, anti-U1RNP, anti-PM/Scl, and anti-Ku [4].

Extracellular vesicles (EVs) are a family of lipid bilayer nanoparticles naturally released from cells into body fluids that act as mediators in cell-to-cell communication convoying cell-specific cargo and influencing various pathophysiological processes [5]. The most prominent nucleic acid molecules enriched in EVs are small RNAs, rarely exceeding 200 base pairs (bp) in length, including regulatory RNAs such as microRNAs (miRNAs), piwi-interacting RNAs (piRNAs) and tRNA-derived small RNA (tsRNAs) [6]. miRNAs are single-stranded small non-coding RNA molecules ranging from 18 to 25 nucleotides (nt) which can target hundreds of messenger RNAs (mRNAs) and regulate several genes. Importantly, cells can selectively sort RNA and miRNA molecules into EVs for secretion and this content is markedly different compared to the parent cell [7,8].

EVs are sources of self-antigens and immune complexes sustaining their likely role in autoimmune diseases [9]. EVs have been proposed as promising biomarkers in Systemic Lupus Erythematosus (SLE), rheumatoid arthritis (RA), primary Sjögren syndrome (pSS), and systemic sclerosis (SSc) [10–12]. The analysis of EVs cargo might provide insights into disease pathogenesis and phenotyping [12]. Indeed, EV-miRNAs are proposed as new non-invasive biomarkers thanks to their high stability, concentration, and integrity coupled with tissue specificity. However, the current knowledge of the role of EVs and EV-miRNAs in IIM is still limited.

The aim of this cross-sectional study was to explore the composition of circulating EVs in IIM, thereby assessing potential differences across IIM subsets heralding peculiar underlying pathogenic mechanisms. Particularly, we aimed at isolating and quantifying the plasma EVs. Subsequently, we explored EVs cargo throughout IIM subsets, with a specific focus on small non-coding RNAs (sncRNAs).

2. Materials and Methods

2.1. Patients

Consecutive adult (≥18 years old) patients fulfilling EULAR/ACR classification criteria for IIM [2] and Connors' [13] and Solomon's [14] criteria for ASyS and followed-up at the Unit of Rheumatology of Padua University Hospital and age- and sex-matched healthy donors (HD) were enrolled in the study. Patients were excluded if they required dialysis or presented with terminal muscle wasting leading to cachexia. PM and ASyS were considered as one group for the purpose of the analysis. CAM was analyzed separately, due to its peculiar pathogenesis [3]. Subjects classified as HD were not on any chronic medication at the time of enrollment and were never diagnosed with any autoimmune diseases or cancer.

This study was conducted in accordance with the Declaration of Helsinki and approved by the local ethics committee (protocol code 5349/AO/22) and did not interfere with good clinical practice. All participants gave written informed consent to study enrolment and data analysis.

2.2. Clinical and laboratory data collection

Demographics, clinical, laboratory, and treatment variables were recorded at the time of patient evaluation. The anonymity of the samples was ensured by using a randomly generated personal identification code. Laboratory data included routine laboratory assessments and levels of muscle enzymes (creatin-phosphokinase, lactate-dehydrogenase, aldolase, myoglobin, aspartate aminotransferase) obtained the same day or at the closest timepoint prior (10 (2–25) days), median IQR) to patient examination. Clinical manifestations of IIM were considered active if present at the time of patient evaluation. Patients not displaying clinically overt manifestations nor laboratory abnormalities related to IIM were considered in remission. MAAs and MSAs antibody specificities were considered positive if retrieved at least once during patient history. Ongoing medications at the time of patient examination were reported.

2.3. Human platelet-free plasma collection

Peripheral blood venous samples were collected from non-fasting subjects in sodium-citrate tubes and platelet-free plasma (PFP) was prepared within 1 h. Briefly, the blood samples in Vacutainer tubes were centrifuged at 1500×*g* for 20 min to separate plasma from cells, and then plasma supernatants were transferred into clean tubes and centrifuged twice at 3000×*g* for 15 min to remove platelets. PFP samples were aliquoted leaving a residue of plasma above the pellet area and stored at −80 °C.

2.4. EVs isolation and quantification

EVs were isolated from human plasma through size-exclusion chromatography (SEC) and ultrafiltration (UF), as recently described [15].

2.4.1. Size-exclusion chromatography (SEC)

PFP samples were defrosted at room temperature to perform the EVs isolation steps. The SEC procedure was performed using qEV original®/70 nm columns (Izon Science, Oxford, UK), following the manufacturer's instructions. Briefly, the Izon column was removed at +4 °C and the column was equilibrated with Phosphate Buffered Saline (PBS) (ThermoFisher Scientific, Waltham, MA, USA) filtered through a 0.22 μm filter unit (Millex - GP; Merck Millipore) (fPBS). Then, 0.5 mL of the PFP sample was added on the top, and fPBS was added to keep it from drying out, subsequently subdividing the eluate into 25 fractions, each one of 0.5 mL. Fractions 1–6 (3 mL) were the void volume which was disposed of. Fractions 7–10 (2 mL) containing the vesicular fraction were collected for further processing, and fractions 11–25 (7.5 mL) containing the protein fraction were eliminated.

2.4.2. Ultrafiltration (UF)

The EVs fractions collected by SEC were enriched through UF using an Amicon® Ultra-4 mL, 100 KDa centrifugal filter unit (Merck Millipore, Billerica, MA, USA). Each filter was sterilized by centrifugation with ethanol 70 % at 2800×*g* for 1 min. The ethanol residues were removed by inversion and then by centrifugation with fPBS at 2800×*g* for 2 min. EVs SEC fractions were added above the previously ethanol-sterilized filter and centrifuged at 4000×*g* for 10 min, according to the manufacturer's instructions, to collect the samples held on the filter containing particles of ≥100 KDa, including EVs, and remove particles of <100 KDa that pass through the filter. The collected samples were

adjusted to a 0.5 mL volume by adding fPBS and frozen at −80 °C.

2.4.3. Nanoparticle Tracking analysis (NTA)

EVs quantification and size were measured in samples diluted in fPBS to the concentration range of 10^6-10^8 particles/mL using the NanoSight NS300 (Malvern Panalytical, UK) instrument, as specified by the manufacturer. The ideal detection threshold was determined to include particles with the restriction concentrations of 20–120 particles per frame, while indistinct particles were limited to 5 per frame. According to the manufacturer's manual, the camera level was increased to visibly distinguish all particles not exceeding a particle signal saturation over 20 % and autofocus was adjusted to avoid indistinct particles. For each sample, particles moving under Brownian motion were recorded on three 1 min videos captured with a 20 × magnification. EVs concentration and size were calculated using NTA software (version 3.4). To minimize data skewing based on single large particles, the ratio between total valid tracks and total complete tracks was always ≤1:5.

2.5. Imaging flow-cytometry

Advanced imaging flow cytometry conducted through Amnis ImageStreamX MkII (ISx; EMD Millipore, Austin, TX, USA) instrument was also employed to perform phenotypic profiling of isolated EVs [15].

2.6. RNA extraction and quantification

Total RNA was extracted from EVs samples using the miRNeasy Serum/Plasma Advanced kit (Qiagen, Germany), according to the manufacturer's protocol. RNA was eluted in 20 μL of RNase-free water and then stored at −80 °C.

2.6.1. miRNAs quantification

MiRNAs concentration (ng/μL) was determined by Qubit microRNA assay kit (Thermo Fisher Scientific, Massachusetts, USA) and measured by Qubit® 4.0 Fluorimeter (Thermo Fisher Scientific, Massachusetts, USA) according to the manufacturer's protocol.

2.7. sncRNA NGS libraries preparation

Universal cDNA synthesis and library preparation of sncRNAs from EVs samples was obtained using QIAseq® miRNA Library kit (Qiagen, Germany), as previously described [16]. Briefly, in an unbiased reaction, universal cDNA synthesis was performed using reverse transcription (RT) primer containing an integrated Unique Molecular Index (UMI) to assign a UMI to every sncRNA molecule, and a universal sequence was added for the sample indexing primers during library amplification. Pre-sequencing and post-sequencing quality control analyses were performed. sncRNA libraries were analyzed by LabChip GX Touch Nucleic Acid Analyzer (PerkinElmer, Massachusetts, USA). We obtained typical electropherograms from sncRNA libraries that show a peak between 170 and 180 bp corresponding to miRNA-sized library and a smaller peak approximately of 188 bp corresponding to a piRNA-sized library.

2.7.1. Small RNA library quantification

NGS library concentration was determined by Qubit dsDNA HS assay (Thermo Fisher Scientific, Massachusetts, USA) by Qubit® 4.0 Fluorimeter, according to the manufacturer's protocol. The concentration of each small RNA Library was expressed in ng/μL and then, converted in molarity (nM).

2.8. sncRNA Next-generation sequencing

Libraries were pooled at equimolar concentrations for multiplexed sequencing.

PhiX DNA 1.5 pM was added to pooled libraries prior to sequencing at a final concentration of 10 % in order to increase the sequence diversity of the libraries. Pooled small RNA libraries (1.7 pM) were sequenced using NextSeq™ 550 System (Illumina, San Diego, California, USA) following manufacturer's instructions. NextSeq 500/550 High Output Kit v2.5 (75 Cycles) was used for sequencing in single reads of 75 pb fragments for small RNA library. This flow cell allows generating around 400 million reads per run, therefore 45 libraries per run were loaded to guarantee around 9 million reads per sample. Calculation of qualitative scores of the NGS runs (cluster density, Passing Filter clusters, % PF, and Q-score) was done with the Real-Time Analysis software (Illumina) and checked by using the Illumina Sequencing Analysis Viewer (Illumina). In our experiments, we obtained 9283.46 ± 18.2 Kreads/sample, with an optimal cluster density (237 ± 1.23 K/mm2), high % PF (86.67 ± 0.32) and Q30 (Q-Score) with an average value of 92.44 % ± 0.02. Finally, the data were collected as FastQ files.

2.9. Bioinformatic analysis of small non-coding RNA

Reads in Fastq files were processed using CLC Genomics Workbench 23.0.5 (Qiagen, Hilden, Germany), a bioinformatic software that provides specific pipelines for small RNAs analysis. Adapter sequences were trimmed and sequences with less than 15bp or without adapter nor UMI (Unique Molecular Index) were discarded. A sequential alignment strategy was used to map sequences on several databases: reference GRCh38 human genome was used, miRBase v.22.1 was considered the first annotation model [17], and sequences were collected as mature miRNAs. Before normalization and differential expression (DE) analysis, data were filtered, considering small RNAs with a minimum number of reads count (mean read count>2.5/group). DE analysis was performed using Generalized Linear Model (GLM) and Trimmed mean of M-values (TMM) normalized counts (CPM) were used as input data, considering significant Benjamini-Hochberg adjusted p-values (p) ≤ 0.05. Sequences that do not match with miRBase annotated sequences were aligned for analysis with piRBase v.3 (https://academic.oup.com/nar/article/50/D1/D265/6454285) for PiwiRNAs, and Dashr v.2 for other classes of sncRNAs [18,19]. All sequences were deposited into the GEO database (http://www.ncbi.nlm.nih.gov/geo/) under accession number GSE247816.

2.10. Putative gene targets for miRNA network analysis

Gene Targets for candidate miRNAs were identified and compared using a bioinformatic tool with an online target prediction algorithm, miRWalk 3.0 (http://zmf.umm.uniheidelberg.de/apps/zmf/mirwalk 2/index.html) a suite of 13 existing miRNA-target prediction programs. Target genes for these miRNAs were selected using gene set enrichment analysis (GSEA) through gene ontology (GO) functional analysis and Gene Ontology biological process (GOBP); for the enrichment analysis, we implemented the results using Search Tool for the Retrieval Interacting Genes (STRING v11.5), and clustering the network targets on high-throughput text-mining. To create the visualization summary networks Cytoscape v3.9.0 was used.

2.11. Statistical analysis

Data were expressed as mean ± standard deviation (SD) or median (interquartile range) for continuous variables while categorical data were expressed as numbers and percentages. A Shapiro–Wilk test was performed to test normality. Student's *t*-test or Mann-Whitney *U* test were used to compare parametric variables, according to distribution. For analysis across multiple miRNAs, raw p-values were corrected for multiple testing by the Benjamini-Hochberg, adjusted p-values (p) ≤ 0.05. Pearson's or Spearman correlation was used to evaluate the strength and direction of the correlation as appropriate. A two-tailed p ≤ 0.05 was considered statistically significant. Data were analyzed using SPSS software version 20.0 (SPSS, Chicago, IL, USA) and GraphPad Prism® version 9 (GraphPad software, CA, USA). ROC analysis was

performed using MedCal ver 19.1.5 (MedCalc Software Ltd, Belgium). Power analysis for NGS data was computed as previously [20]. Sample size was estimated to be at least 12 subjects per group to reach the desired power of 80 %, with a SD estimated at 0.5, an average power with FDR of 0.05 and fold change of 1.3.

2.12. Data and Resource Availability

The data sets generated and/or analyzed during this study are available from the corresponding author on reasonable request.

3. Results

3.1. Patients cohort

Forty-seven IIM patients (female:male ratio 2:1, mean age 59.62 ± 13.55 SD) and 45 age- and sex-matched HD (female:male ratio 2:1, mean age 54.65 ± 16.86) were included in the present study who underwent RNA extraction and small non-coding RNAs analysis following EVs isolation, quantification, and characterization. IIM patients were distributed across different groups encompassing CAM and non-CAM subsets, whose clinical and demographic parameters are reported in Table 1. CAM patients in our cohort were affected with ovary carcinoma (n = 1), lung adenocarcinoma (n = 2), colon cancer (n = 3), adenocarcinoma of the pancreas (n = 1), biliary tract (n = 1), large intestine (n = 1), intestinal-type of the left nasal cavity (n = 1), breast non-Hodgkin lymphoma (n = 1), and carcinoma of the forehead (n = 1). Muscle enzyme values across HD were within the range of normality for the general population (data not shown).

3.2. sncRNome of characterized circulating EVs in IIM patients

Circulating EVs were isolated and characterized from IIM patients and HD controls. Imaging flow cytometry characterization confirmed the presence of EVs bearing acknowledged tetraspanin markers (CD9, CD63, CD81) (Supplementary Fig. 1). No significant difference in the mean concentration of EVs and in the EVs mode size were found between non-CAM-IIM patients and HD. (Fig. 1A).

Next, we performed a sncRNome by NGS from circulating EVs. Sequences in the typical range size of 15–55 nucleotides (nt) were considered sncRNA transcripts. The bioinformatics analysis showed that among the 2.632 miRNAs aligned, 519 were expressed in both groups at least in one sample. After filtered correction, the bioinformatics analysis covered 109 miRNAs (Fig. 1B). A heat map of the 50 most expressed miRNAs is reported in Supplementary Fig. 2.

Next, we analyzed the levels of these 109 miRNAs in EVs from IIM and HD. Principal component analysis (PCA) showed that their expression profile well discriminated between patients and HD. (Fig. 1C). The volcano plot in Fig. 1D shows significantly and differentially expressed miRNAs in IIM compared to HD.

After filtering correction, four miRNAs (miR-486-5p, miR-122-5p, miR-192-5p, miR-32-5p) were up-regulated (Fig. 2A), and four miRNAs (miR-142-3p, miR-141-3p, let-7a-5p and miR-3613-5p) were down-regulated in EVs of IIM in comparison to HD (Fig. 2B). Receiver operating characteristic curve (ROC) analyses were performed to determine the power capacity of the eight selected miRNAs to discriminate between patients with IIM patients and HD: miR-486-5p and miR-142-5p show the best performance respect to the other miRNAs with the areas under the curve (AUC) 0.74 and 0.79, respectively (Fig. 2C–Supplementary Table 1).

We also assessed the differential expression (DE) analysis of other mainly expressed classes of sncRNAs in our samples, in IIM patients compared to HD. piRNA DE analysis shows that 3 piRNAs were significantly upregulated and 3 piRNAs were significantly downregulated in EVs from IIM patients in comparison to HD (Supplementary Fig. 4A).

Table 1
Clinical characteristics of the patients' cohort.

Clinical and demographic features	Values
Patients (n)	47
Females (n, %)	30 (63.83)
Caucasians (n, %)	47 (100)
Disease duration at sampling time (years)	4.70 ± 4.98
MMT-8 score median (IQR)	144 (100–150)
Serology (n, %)	
Myositis-specific autoantibodies (MSAs)	33 (70.21)
Anti-Mi2	6 (12.76)
Anti-*t*-RNA synthetase *	15 (31.91)
Anti-SRP	3 (6.37)
Anti-MDA-5	4 (8.51)
Anti-TIF1-γ	4 (8.51)
Anti-HMGCoAR	1 (2.13)
Myositis-associated autoantibodies (MAAs)	20 (42.55)
Anti-SSA	10 (21.28)
Anti-SSB	2 (4.25)
Anti-Ku	1 (2.13)
Anti-PM/Scl-100	3 (6.37)
Other **	4 (8.51)
Unknown	1 (2.13)
IIM subsets (n, %)	
Non-cancer-associated myositis (CAM)	35 (74.46)
Dermatomyositis (DM)	14 (29.79)
Polymyositis (PM)	6 (12.76)
Anti-synthetase syndrome (ASyS)	15 (31.91)
Cancer-associated myositis (CAM)	12 (25.52)
Active clinical manifestations upon sampling (n, %)	
Cutaneous	22 (46.81)
Gottron's sign and papules	10 (21.28)
Heliotropic rash	6 (12.76)
Other ***	20 (42.55)
Arthritis	5 (10.64)
Myositis	15 (31.90)
Interstitial lung disease (ILD)	7 (14.88)
Clinical remission	40 (85.11)
Myositis-related laboratory (U/L)	
Creatine phosphokinase (CPK)	121.5 (75.75–483.25)
Aldolase	5.4 (5–10.4)
Glutamate oxaloacetate transaminase (GOT)	30 (30–46)
Lactate dehydrogenase (LDH)	215.5 (200–327.25)
Ongoing treatment	
Oral glucocorticoids (n, %)	36 (76.59)
Dose of prednisone (mg/day)	12.5 (0–25)
Immunosuppressant drugs (n, %)	28 (59.57)
Mycophenolate mofetil	12 (25.52)
Methotrexate	9 (19.15)
Azathioprine	1 (2.13)
Cyclosporine A/Tacrolimus	2 (4.25)
Rituximab	3 (6.37)
Abatacept	1 (2.13)
Untreated (n, %)	3 (6.37)

Anti-*t*-RNA synthetase *: 10 cases of anti-Jo1 positivity (21.28 %), 4 cases of anti-PL12 positivity (8.51 %), 1 case of anti-PL7 positivity (2.13 %). Other **: 1 case of anti-U1RNP (2.13 %), 3 cases of anti-PM/Scl-75 positivity (6.37 %). Other ***:7 cases with shawl rash (14.88 %), 3 cases with holster sign (6.37 %), 5 cases with nailfold changes (10.64 %), 6 cases with mid-facial erythema (12.76 %), 4 cases with V-neck sign (8.51 %), 8 cases with mechanics's hands (17.02 %).
Normal values for reference of myositis-related laboratory: CPK: 20–180 U/L; Aldolase: 1.0–7.7 U/L; GOT: 6–42 U/L; LDH: 135–214 U/L.
MMT-8: Manual Muscle Test-8; IQR: interquartile range; Anti-*t*-RNA synthetase: Anti-transfer RNA synthetases; Anti-SRP: Anti-signal recognition particle; Anti-MDA-5: Anti-melanoma differentiation-associated gene 5; Anti-TIF1-γ: Anti-transcriptional intermediary factor 1-γ antibody; Anti-HMGCoAR: Anti-hydroxy-methyl-glutaryl-coenzyme A reductase; Anti-SSA: Anti–Sjögren's-syndrome-related antigen A; Anti-SSB: Anti–Sjögren's-syndrome-related antigen B. Values are expressed as median IQR.

3.3. miRNA gene targets network analysis

To gain insight into the functional role of selected miRNAs in IIM patients, we analyzed their potential gene targets enriched in

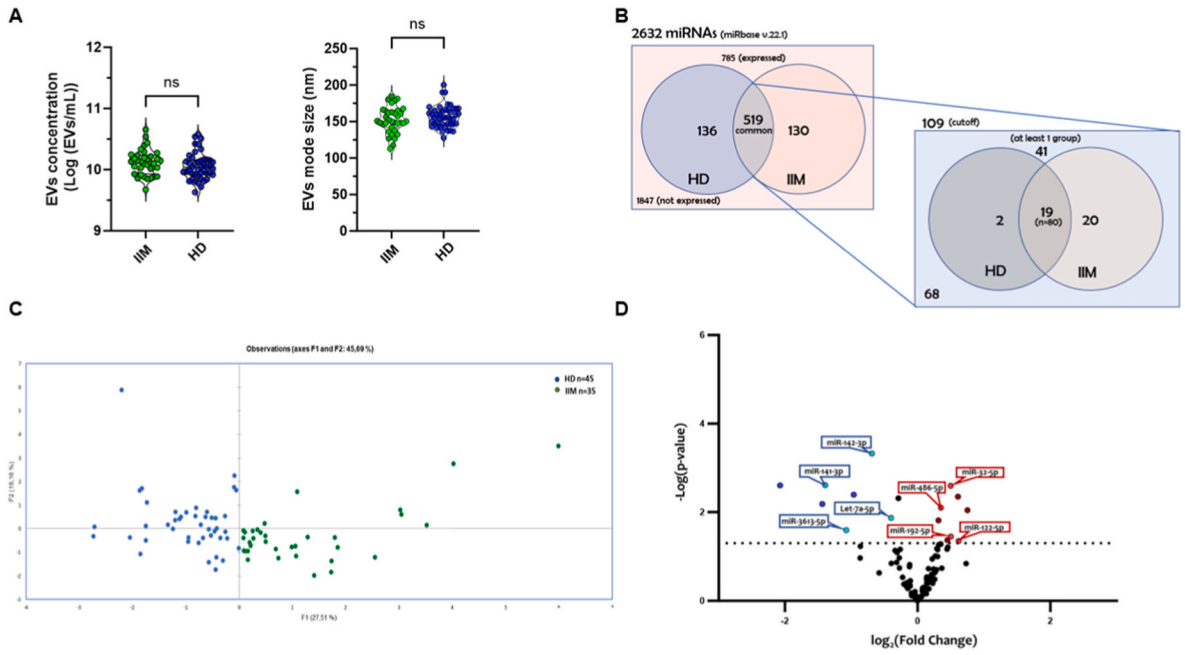

Fig. 1. miRNome of characterized circulating EVs in IIM patients vs HD. ***(A)*** Violin plot representing the circulating EVs concentration (Log [EVs/mL]) (on the left) and EVs mode diameter (nm) (on the right) in IIM (n = 35) vs. HD (n = 45)***; (B)*** Venn diagram shows the number of miRNAs aligned through bioinformatic analysis (2,632) and their distribution across EVs samples and condition (HD and IIM patients). Among 519 miRNAs expressed in both groups (at least one read detected in at least one sample per group), miRNAs with an average read count cutoff of ≥2.5/group and expressed at least in 30 samples per group were retained for DE analysis between the two groups (109 miRNAs): 41 miRNAs were expressed at least in all of the samples of one group (HD and/or IIM), of which 19 miRNAs were consistently expressed in all of the samples of the cohort (n = 80); ***(C)*** Unsupervised principal component analysis of the EV miRNA expression profiles in IIM patients (green dots) and HD (blue dots) samples; ***(D)*** Volcano plot of 109 miRNAs analyzed for DE. Horizontal line delineates adjusted $p < 0.05$ by Benjamini-Hochberg procedure, and blue dots indicate downregulated miRNAs and red dots upregulated miRNAs.

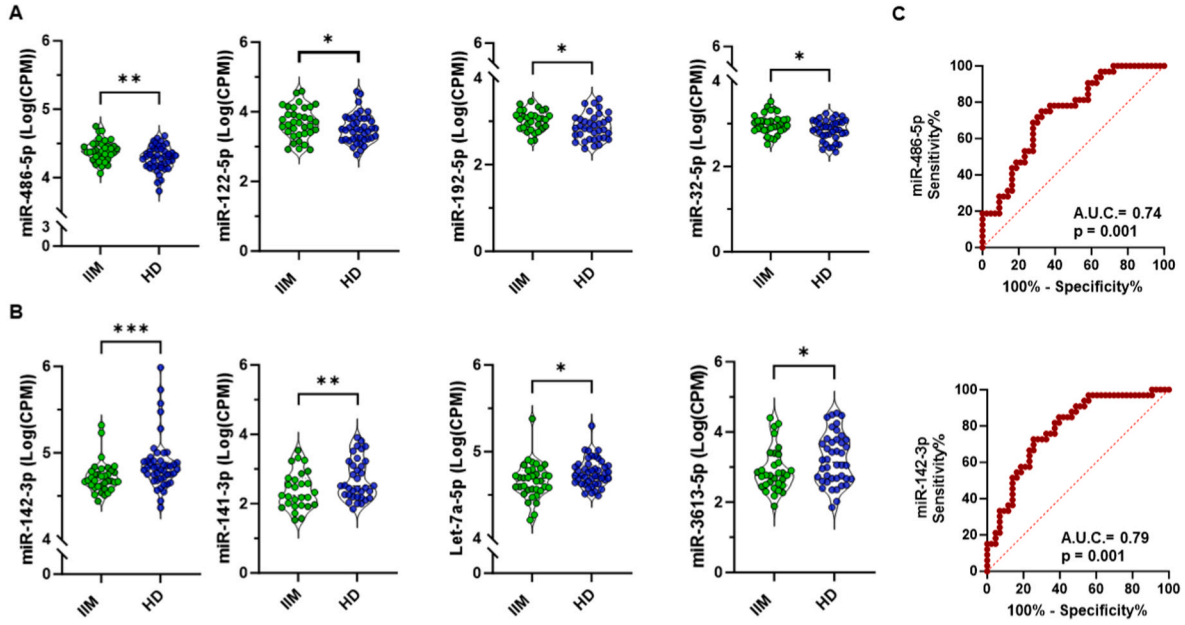

Fig. 2. Differentially expressed circulating EV-miRNAs in IIM vs HD. Violin plots of candidate upregulated ***(A)*** and downregulated ***(B)*** circulating miRNAs in EVs of IIM patients compared to HD; ***(C)*** Receiver operating characteristic curve (ROC) for prediction of IIM based on the expression of miR-486-5p or miR-142-5p; A.U.C. (Area Under the Curve). miRNA expression is reported as counts per million reads (CPM). Groups include IIM (n = 35, green dots) and HD (n = 45, dark blue dots). *$p < 0.05$, **$p < 0.01$, ***$p < 0.001$ *t*-test for unpaired data.

inflammatory myopathies, such as inflammation and interferon pathways, necroptosis and hypoxia pathways. Using Cytoscape, we created a biological network showing the match of predictive targets for upregulated miRNAs (Fig. 3A and B) and the downregulated miRNAs (Fig. 3C and D) in patients with IIM and their primary biological process.

We found that several target genes for upregulated and downregulated miRNAs in subjects with IIM are implicated in apoptosis, cell differentiation and activation, necroptosis and inflammation. Among

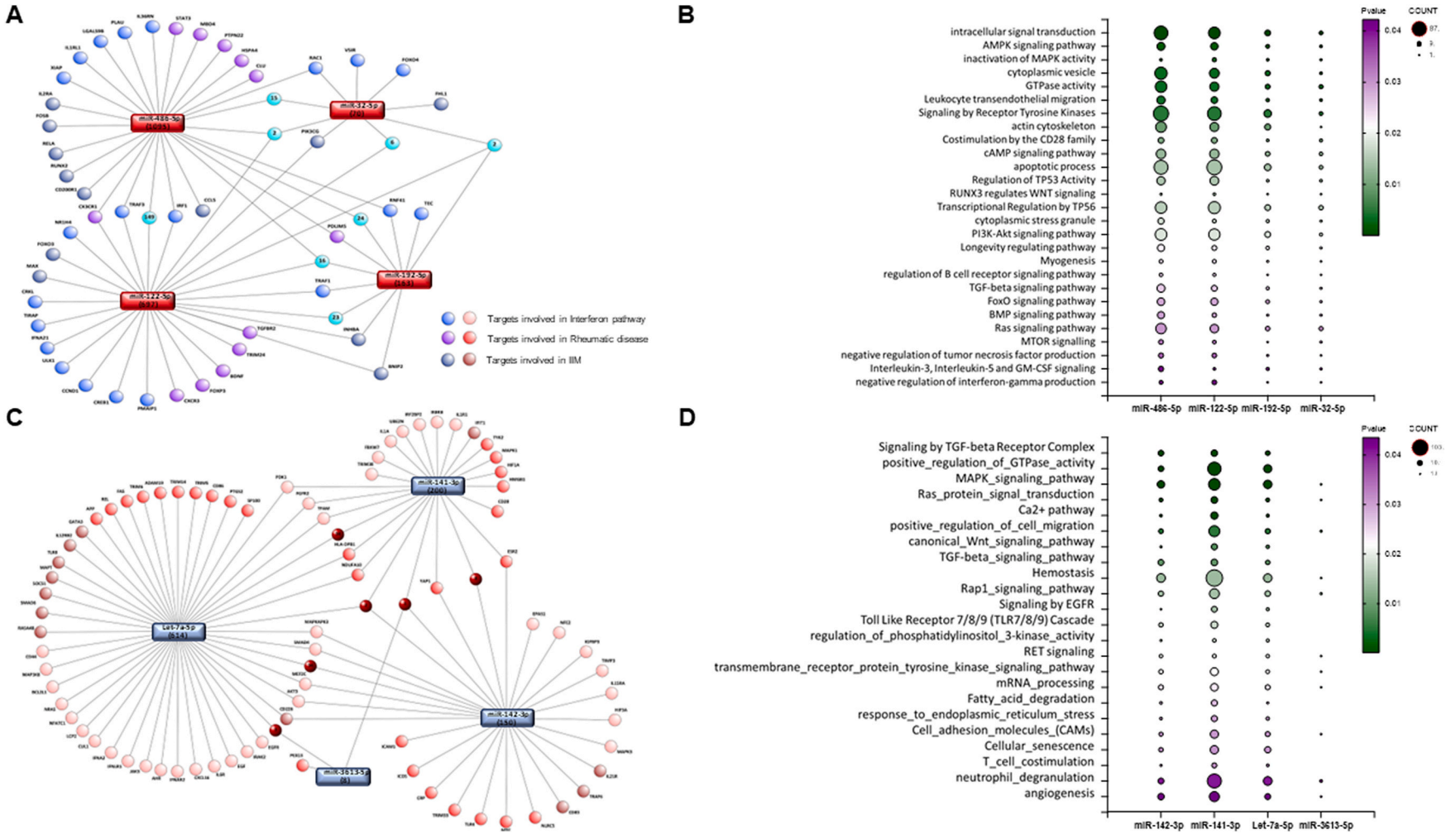

Fig. 3. Signaling networks of EV-derived miRNAs in IIM. Networks of putative target genes for circulating EV-derived miRNAs upregulated ***(A)*** and downregulated ***(C)*** in IIM patients vs. HD and their relative bubble graphs describing respectively the most significant enriched pathways ***(B, D)***. Target gene identification, selection and network visualization are described in the Methods section. Upregulation of miRNAs/target genes are indicated as red squares/dots; downregulation of miRNAs/target genes are indicated as blue squares/dots; numerical value represents the number of putative target genes for each miRNA. In bubble graph, the bubble size represents a relative scale of the number of putative target genes involved in the biological process for each miRNA.

significantly enriched pathways, cytoplasmic vesicles, leukocyte transendothelial migration, apoptotic process and signaling by receptor tyrosine kinases are widely reported to be related to the development and progression of IIM disease.

3.4. EV-derived sncRNAs in non-CAM-IIM subtypes

To straighten out the pathological role of EV-miRNA content across IIM subtypes, we further analyzed sncRNA expression distinguishing non-CAM-IIM diagnosis (DM, ASyS, PM). No significant difference in mean concentration or size of circulating EVs was shown across IIM subsets (Fig. 4A, top). DE analysis of sncRNA sequencing data obtained from EVs of DM and non-DM revealed two miRNAs which were significantly differential expressed: miR-335-5p was up-regulated in DM group, while miR-27a-3p was significantly downregulated in DM group in comparison to non-DM group (Fig. 4B, top). ROC curve analysis shows that miR-335-5p has a sensitivity of 0.90 and specificity of 0.71 with AUC of 0.82 ($p = 0.001$), while miR-27a-3p has a sensitivity of 0.71 and specificity of 0.71 with AUC of 0.75 ($p = 0.005$) (Fig. 4C) in separating DM and non-DM patients. Among other sncRNA DE analysis we found piRNA-has-165252 to be significantly upregulated in DM group in comparison to non-DM group (Supplementary Fig. 4B).

3.5. EV-derived sncRNAs in CAM

CAM represent a peculiar IIM subset burdened with significant morbidity and mortality, with a distinguished genetic background [3]. We separately determined the amount of EVs and sncRNAs EV content in CAM patients as compared to non-CAM-IIM. We analyzed CAM patients separately from non-CAM patients to determine the amount of EVs and sncRNAs EV content.

Levels of circulating EVs were significantly increased in CAM in comparison to non-CAM IIM ($2.62 \times 10^{10} \pm 2.48 \times 10^{10}$ vs. $1.48 \times 10^{10} \pm 8.19 \times 10^{9}$, $p = 0.0198$) and HD ($2.62 \times 10^{10} \pm 2.48 \times 10^{10}$ vs. $1.30 \times 10^{10} \pm 7.69 \times 10^{9}$, $p = 0.0029$), while no difference was observed for EVs mode size (Fig. 4A, bottom and Supplementary Fig. 3).

EV-derived sncRNAs sequencing showed that let-7f-5p was upregulated while miR-143-3p was downregulated in CAM patients in comparison to non-CAM-IIM patients (Fig. 4B, bottom). ROC curve analysis showed that let-7f-5p and miR-143-3p had a good performance of specificity and sensitivity for CAM. The AUC values for let-7f-5p and miR-143-3p were 0.81 and 0.74, respectively (Fig. 4D). Finally, DE analysis of other sncRNAs reveal significant differences in piRNA expression between the two groups, with three piRNAs significantly downregulated in CAM patients in comparison to non-CAM-IIM (Supplementary Fig. 4C).

3.6. Correlation with laboratory biomarkers

An inverse correlation was observed between EV levels and CPK ($r = -0.4181$; $p = 0.0038$), aldolase ($r = -0.3757$; $p = 0.0184$), and LDH ($r = -0.3598$; $p = 0.0431$) (Supplementary Fig. 5). The analysis of the correlations between the miRNA expression and the clinical parameters revealed that miR-486-5p was positively correlated with the level of CPK ($r = 0.43$, $p = 0.01$) and myoglobin ($r = 0.38$, $p = 0.022$), miR-122-5p with the level of myoglobin ($r = 0.24$, $p = 0.043$) and with AST ($r = 0.36$, $p = 0.02$) and with ALT ($r = 0.38$ $p = 0.018$).

4. Discussion

In this study, we report a comprehensive sncRNA analysis by small RNA-Seq in circulating EVs from matching samples of IIM patients and HD. Our main findings show that four miRNAs, namely miR-486-5p, miR-122-5p, miR-192-5p, miR-32-5p were significantly upregulated, while four miRNAs, namely miR-142-3p, miR-141-3p, let-7a-5p and miR-3613-5p, were downregulated in IIM. We also identified another

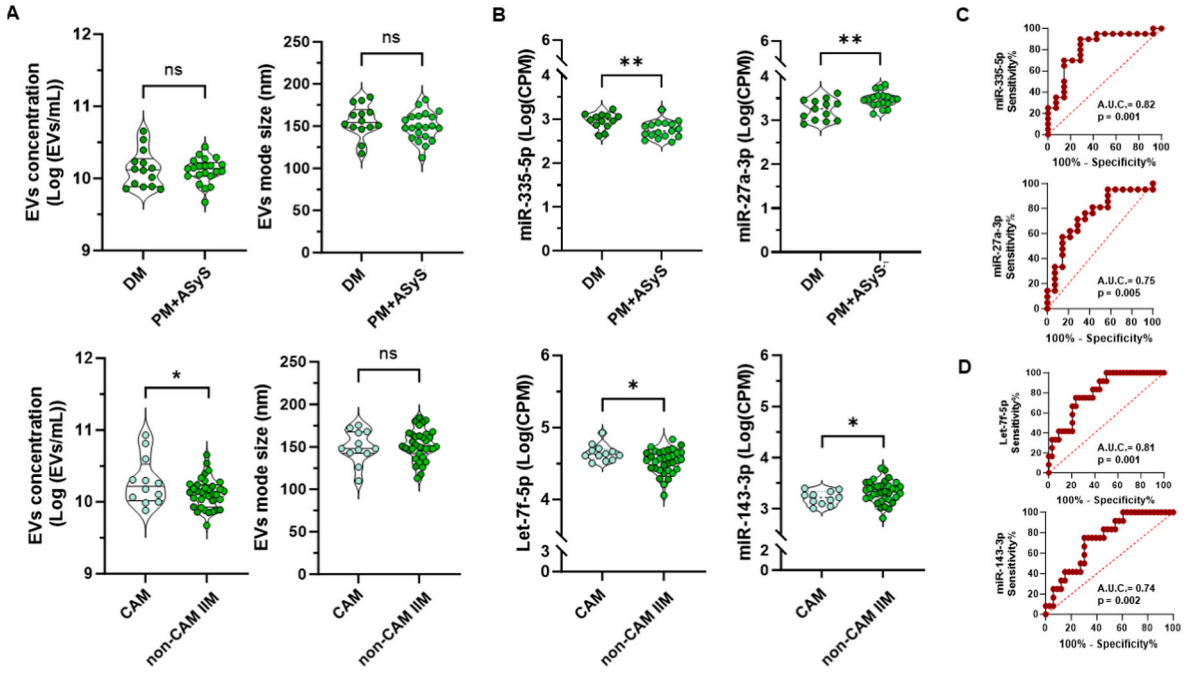

Fig. 4. EVs and their miRNA-cargo in IIM subtypes and CAM. ***(A)*** On the top, violin plot representing the circulating EVs concentration (Log [EVs/mL]) (on the left) and EVs mode diameter (nm) (on the right) in (dermatomyositis) DM (n = 14) vs. ASyS + PM (n = 21). On the bottom, violin plot representing the circulating EVs concentration (Log [EVs/mL]) (on the left) and EVs mode diameter (nm) (on the right) in IIM (n = 35) vs. CAM (n = 12)***; (B)*** On the top, violin plots of candidate circulating EV-miRNAs differentially expressed in DM vs. non-DM group (ASyS + PM). On the bottom, violin plots of candidate circulating EV-miRNAs differentially expressed in CAM vs. IIM patients; ***(C)*** Receiver operating characteristic curve (ROC) for prediction of IIM subtypes based on the expression of miR-335-5p or miR-27a-3p; A.U.C. (Area under the curve); ***(D)*** ROC for prediction of CAM patients based on the expression of let-7f-5p or miR-143-3p. miRNA expression is reported as counts per million reads (CPM). *$p < 0.05$, **$p < 0.01$ *t*-test for unpaired data.

class of sncRNA, i.e. piRNAs differentially expressed in EVs between IIM patients and HD. The bioinformatic analysis of miRNA gene target network showed that these EV-derived miRNAs target the expression of several genes which modulate inflammatory, necroptosis, interferon and immune signaling. Finally, we observed higher levels of EVs and different expression of EV-sncRNAs from CAM compared to non-CAM-IIM.

A recent study conducted on plasma EV-miRNAs cargo by RNA-Seq technology only evaluated DM patients comparing them with HD [21]. Further studies of circulating miRNAs focused on DM/PM [22] and sporadic IBM [23] are characterized by small size population and used microarrays and reverse transcription polymerase chain reaction technologies. Other evidence has revealed a different miRNA expression profile in muscle biopsies from heterogeneous groups of IIM patients, but none included CAM patients [24,25]. To the best of our knowledge, this is the first study on circulating EVs cargo which identifies sncRNAs as important biomarkers of disease and as mediators of specific molecular pathways across different IIM subsets.

IIM are a group of rare disorders affecting skeletal muscle as well as several organ systems [1,2]. Both innate and adaptive immune processes are known to have a role in IIM; however, the mechanisms responsible for initiation and progression of IIM remain elusive. Muscle inflammation and damage might lead to EVs release able to modulate immune responses and pathophysiological processes [26].

EVs regulate intercellular communications by transferring cytosolic proteins, lipids, and nucleic acids [5,10]. Due to their persistence in the circulation system, they are potential non-invasive markers for disease progression or treatment. Growing evidence attests the contribution of EVs and miRNA cargo to aberrant inflammatory and autoimmune responses [26], including SLE, RA and SS [10–12,27,28].

In this study we showed a set of miRNAs differentially expressed in EVs from IIM in comparison to HD. In detail, the upregulated miR-486-5p and the downregulated miR-142-3p provided a remarkable discrimination between IIM and HD, thereby submitting their role as potential contributors and biomarkers for the development of IIM. miR-486-5p belongs to myomiRs, which are involved in myoblast proliferation, differentiation and muscle regeneration [29]. miR-486 is released by muscle cells, modulates key genes involved in apoptosis and inflammation such as STAT3, HSPA4 and PTPN22 and is enriched within EVs [30]. The link between miR-486-5p expression and impaired muscle function is supported by its correlation with CPK and myoglobin levels in our cohort. The down-regulated miR-142-3p plays important role in hematopoiesis and T cell functions [31] and downregulation of miR-142-3p has been found in autoimmune diseases and in several blood cancers [32]. Consistently, our predictive pathway analysis indicates that the reduction of expression of miR-142-3p may alter the regulation of key proteins in the immune and cytokine response (TLR4, ICAM-1, IL-15R and IL21R) and hypoxia pathway (EPAS1, NFE2 and HIF3-alpha) lowering oxygen levels which lead to muscle weakness.

Although the role of miR-32-5p and miR-122-5p have not been investigated in systemic autoimmune diseases yet, their over-expression in IIM were reported in other studies, confirming their role in inflammation and immune pathways [33].

Across IIM, DM was also identified by peculiar miRNA expression characterized by the upregulation of miR-335-5p and downregulation of miR-27a-3p. miR-335-5p is regulated by NF-κB signaling and interferon-γ [34,35], and has been reported to promote proliferation, inhibits apoptosis, and reduces the expression of inflammatory factors by activating autophagy [36–38]. An in vitro study showed that miR-27a targets transcripts in the MAPK signaling pathway, and its transfection lowered the levels of multiple cytokines, including TNF-α, IL-1β, IL-6, IL-12, and IL-23 [39], with a putative anti-inflammatory effect. The subset of cancer-associated myositis (CAM) showed the highest circulating EVs levels sustaining the relationship between cancer and autoimmune dysregulation. In fact, circulating EVs might play a key role as cancer self-propagating products and autoimmunity inductors. A prolonged and extensive antigen presentation through EVs from the cancer milieu could trigger a potent autoimmune response culminating into paraneoplastic myopathic manifestations [40]. CAM was characterized by an enhanced let-7f-5p expression and a decrease of miR-143-3p than non-CAM-IIM.

Let-7f-5p belongs to let-7 family, regulators of both innate and adaptive immune cells [41] and anti-inflammatory mechanisms [42,43]. Its dysregulated expression has been observed in several autoimmune diseases including SLE and SSc [38,44]. Our results suggest let-7f-5p as part of a distinct miRNA signature at the clinical onset of IIM which may be involved in the progressive development of CAM. However, reciprocal modulation of let-7f-5a, inflammation and cancer impose a careful interpretation. miR-143-3p acts as tumour suppressor [45]. Recently, a link emerged between its modulatory effect and the molecular mechanisms associated to necroptosis [46,47], which triggers the release of intracellular components by dead cells, such as EVs [48,49]. In fact, miR-143-3p targets key mediators in cell death pathways and inflammatory signaling. Therefore, the decreased miR-143-3p expression in CAM may suggest a link between cancer progression and this IIM subset.

Very few studies have assessed the level of EV-piRNAs in IIM. piRNAs protects genome integrity, are mainly found in germline cells, heart, nervous system, immune cells and plasma [50,51]. Several reports show that piRNAs are associated with various disease, such as inflammation and cancer [52,53]. Our data indicate that piRNAs are contained in EVs and several piRNAs are differentially expressed in IIM patients, suggesting a potential involvement in transcriptional and post-transcriptional changes, thereby affecting immune cell differentiation and secretion of inflammatory mediators. The clinical relevance of these results claims further studies. Our study has some limitations. A limited sample size with heterogeneous manifestations may be insufficient for peculiar analysis, including the potential effect of different treatment regimens or stratification by organ involvement on EVs and miRNAs distribution. Furthermore, longitudinal observations over a cross-sectional design are required to determine the impact of immunosuppressive treatment on EVs release and sncRNAs content. Last, mechanistic assays are required to explore the functional role of miRNAs and piRNAs in IIM.

5. Conclusions

Overall, we showed for the first time a set of miRNAs and piRNAs derived from EVs differentially expressed in IIM patients and related to impaired muscle function and cell survival. Among IIM subsets, CAM and DM disclosed a peculiar epigenetic footprint. Our findings could have important clinical implications in phenotyping of IIM patients at disease onset and informing about further disease development and outcome.

CRediT authorship contribution statement

Chiara Franco: Conceptualization, Data curation, Formal analysis, Investigation, Methodology, Project administration, Software, Visualization, Writing – original draft, Writing – review & editing. **Alessandra Giannella:** Conceptualization, Data curation, Formal analysis, Investigation, Methodology, Project administration, Software, Writing – original draft, Writing – review & editing. **Michela Gasparotto:** Resources, Visualization. **Elisabetta Zanatta:** Resources. **Anna Ghirardello:** Methodology. **Federico Pettorossi:** Data curation, Resources. **Zahrà Rahmè:** Data curation, Resources. **Roberto Depascale:** Data curation, Resources. **Davide Ragno:** Methodology, Software. **Gioele Bevilacqua:** Visualization. **Elisa Bellis:** Visualization. **Luca Iaccarino:** Resources, Supervision. **Andrea Doria:** Conceptualization, Project administration, Supervision, Writing – original draft, Writing – review & editing. **Giulio Ceolotto:** Conceptualization, Data curation, Formal analysis, Investigation, Methodology, Project administration, Software, Supervision,

Visualization, Writing – original draft, Writing – review & editing. **Mariele Gatto:** Conceptualization, Data curation, Formal analysis, Investigation, Project administration, Software, Supervision, Visualization, Writing – original draft, Writing – review & editing.

Declaration of competing interest

The authors have no conflict of interest in context of this manuscript.

Acknowledgments

The authors thank P. Mosca, Medicine Department, University of Padova, Italy, for bioinformatic assistance. RNA-seq was performed by Illumina, United States, NextSeq 550 instrument which was purchased by the DIMAR Excellence project funding (DImed and MAlattie Rare) of the Department of Medicine, University of Padua.

Appendix A. Supplementary data

Supplementary data to this article can be found online at https://doi.org/10.1016/j.jaut.2024.103255.

References

[1] J. Tanboon, A. Uruha, W. Stenzel, I. Nishino, Where are we moving in the classification of idiopathic inflammatory myopathies? Curr. Opin. Neurol. 33 (5) (2020) 590–603, https://doi.org/10.1097/WCO.0000000000000855.
[2] I.E. Lundberg, A. Tjärnlund, M. Bottai, V.P. Werth, C. Pilkington, M. De Visser, et al., EULAR/ACR classification criteria for adult and juvenile idiopathic inflammatory myopathies and their major subgroups HHS Public Access, Ann. Rheum. Dis. 76 (12) (2017) 1955–1964, https://doi.org/10.1136/annrheumdis-2017-211468.
[3] K. Patasova, I.E. Lundberg, M. Holmqvist, Genetic influences in cancer-associated myositis, Arthritis Rheumatol. 75 (2) (2023 Feb 20) 153–163, https://doi.org/10.1002/art.42345.
[4] Martinez M. Loredo, S. Zampieri, C. Franco, A. Ghirardello, A. Doria, M. Gatto, Nonimmune mechanisms in idiopathic inflammatory myopathies, GhirardelloA, Gatto M, Franco C, Zanatta E, Padoan R, Ienna L, et al. Detection of myositis autoantibodies by multi-analytic immunoassays in a large multicenter cohort of patients with definite idiopathic inflammatory myopathies. Diagnostics. 2023;13 (19):1–522, Curr. Opin. Rheumatol. 32 (6) (2020) 515–522, https://doi.org/10.1097/BOR.0000000000000748.5, 10.3390/diagnostics13193080.
[5] M. Yáñez-Mó, P.R.M. Siljander, Z. Andreu, A. Bedina Zavec, F.E. Borràs, E.I. Buzas, et al., Biological properties of extracellular vesicles and their physiological functions, J. Extracell. Vesicles 4 (1) (2015 Jan 1) 27066, https://doi.org/10.3402/jev.v4.27066.
[6] K.M. Kim, K. Abdelmohsen, M. Mustapic, D. Kapogiannis, M. Gorospe, RNA in extracellular vesicles, WIREs RNA 8 (4) (2017 Jul 28) 100–106, https://doi.org/10.1002/wrna.1413.
[7] M. Groot, H. Lee, Sorting mechanisms for microRNAs into extracellular vesicles and their associated diseases, Cells 9 (4) (2020) 1–16, https://doi.org/10.3390/cells9041044.
[8] G. Ceolotto, A. Giannella, M. Albiero, M. Kuppusamy, C. Radu, P. Simioni, et al., MiR-30c-5p regulates macrophage-mediated inflammation and pro-atherosclerosis pathways, Cardiovasc. Res. 113 (13) (2017 Nov 1) 1627–1638, https://doi.org/10.1093/cvr/cvx157.
[9] M. Lu, E. DiBernardo, E. Parks, H. Fox, S.Y. Zheng, E. Wayne, The role of extracellular vesicles in the pathogenesis and treatment of autoimmune disorders, Front. Immunol. 12 (2021 Feb 24) 566299, https://doi.org/10.3389/fimmu.2021.566299.
[10] J. Tian, G. Casella, Y. Zhang, A. Rostami, X. Li, Potential roles of extracellular vesicles in the pathophysiology, diagnosis, and treatment of autoimmune diseases, Int. J. Biol. Sci. 16 (4) (2020) 620–632, https://doi.org/10.7150/ijbs.39629.
[11] B. Zhang, M. Zhao, Q. Lu, Extracellular vesicles in rheumatoid arthritis and systemic lupus erythematosus: functions and applications, Front. Immunol. 14 (2021 Jan) 11, https://doi.org/10.3389/fimmu.2020.575712.
[12] K. Xu, Q. Liu, K. Wu, L. Liu, M. Zhao, H. Yang, et al., Extracellular vesicles as potential biomarkers and therapeutic approaches in autoimmune diseases, J. Transl. Med. 18 (1) (2020 Dec 12) 432, https://doi.org/10.1186/s12967-020-02609-0.
[13] G.R. Connors, L. Christopher-Stine, C.V. Oddis, S.K. Danoff, Interstitial lung disease associated with the idiopathic inflammatory myopathies: what progress has been made in the past 35 years? Chest 138 (6) (2010 Dec) 1464–1474.
[14] J. Solomon, J.J. Swigris, K.K. Brown, Myositis-related interstitial lung disease and antisynthetase syndrome, J. Bras. Pneumol. 37 (1) (2011 Jan-Feb) 100–109, https://doi.org/10.1590/s1806-37132011000100015.
[15] C. Franco, A. Ghirardello, L. Bertazza, M. Gasparotto, E. Zanatta, L. Iaccarino, et al., Size-exclusion chromatography combined with ultrafiltration efficiently isolates extracellular vesicles from human blood samples in health and disease, Int. J. Mol. Sci. 24 (4) (2023 Feb 11) 3663, https://doi.org/10.3390/ijms24043663.
[16] A. Giannella, E. Castelblanco, C.F. Zambon, D. Basso, M. Hernandez, E. Ortega, et al., Circulating small noncoding RNA profiling as a potential biomarker of atherosclerotic plaque composition in type 1 diabetes, Diabetes Care 46 (3) (2023) 551–560, https://doi.org/10.2337/dc22-1441.
[17] P.P. Kuksa, A. Amlie-Wolf, Ž. Katanić, O. Valladares, L.S. Wang, Y.Y. Leung, Dashr 2.0: integrated database of human small non-coding RNA genes and mature products, in: J. Kelso (Ed.), Bioinformatics 35 (6) (2019 Mar 15) 1033–1039, https://doi.org/10.1093/bioinformatics/bty709.
[18] M.G.M. Kok, M.W.J. de Ronde, P.D. Moerland, J.M. Ruijter, E.E. Creemers, S. J. Pinto-Sietsma, Small sample sizes in high-throughput miRNA screens: a common pitfall for the identification of miRNA biomarkers, Biomol Detect Quantif. 15 (August 2017) (2018) 1–5, https://doi.org/10.1016/j.bdq.2017.11.002.
[19] S.N. Hart, T.M. Therneau, Y. Zhang, G.A. Poland, J.P. Kocher, Calculating sample size estimates for RNA sequencing data, J. Comput. Biol. 20 (12) (2013) 970–978, https://doi.org/10.1089/cmb.2012.0283.
[20] L. Li, X. Zuo, D. Liu, H. Luo, H. Zhang, Q. Peng, et al., Plasma exosomal RNAs have potential as both clinical biomarkers and therapeutic targets of dermatomyositis, Rheumatology 61 (6) (2022) 2672–2681, https://doi.org/10.1093/rheumatology/keab753.
[21] T. Hirai, K. Ikeda, H. Tsushima, M. Fujishiro, K. Hayakawa, Y. Yoshida, et al., Circulating plasma microRNA profiling in patients with polymyositis/dermatomyositis before and after treatment: miRNA may be associated with polymyositis/dermatomyositis, Inflamm. Regen. 38 (1) (2018 Dec 8) 1, https://doi.org/10.1186/s41232-017-0058-1.
[22] M. Lucchini, V. De Arcangelis, M. Santoro, R. Morosetti, A. Broccolini, M. Mirabella, Serum-circulating microRNAs in sporadic Inclusion body myositis, Int. J. Mol. Sci. 24 (13) (2023), https://doi.org/10.3390/ijms241311139.
[23] S. Muñoz-Braceras, I. Pinal-Fernandez, M. Casal-Dominguez, K. Pak, J. C. Milisenda, S. Lu, et al., Identification of unique microRNA profiles in different types of idiopathic inflammatory Myopathy, Cells 12 (2023) 2198, https://doi.org/10.3390/cells12172198.
[24] S. Rome, A. Forterre, M.L. Mizgier, K. Bouzakri, Skeletal muscle-released extracellular vesicles: state of the art, Front. Physiol. 10 (2019 Aug 9) 929, https://doi.org/10.3389/fphys.2019.00929.
[25] J.H.W. Distler, D.S. Pisetsky, L.C. Huber, J.R. Kalden, S. Gay, O. Distler, Microparticles as regulators of inflammation: novel players of cellular crosstalk in the rheumatic diseases, Arthritis Rheum. 52 (2005) 3337–3348, https://doi.org/10.1002/art.21350.
[26] E.I. Buzas, The roles of extracellular vesicles in the immune system, Nat. Rev. Immunol. 23 (2023) 236–250, https://doi.org/10.1038/s41577-022-00763-8.
[27] F. Finamore, A. Cecchettini, E. Ceccherini, G. Signore, F. Ferro, S. Rocchiccioli, et al., Characterization of extracellular vesicle cargo in sjögren's syndrome through a SWATH-MS proteomics approach, Int. J. Mol. Sci. 22 (9) (2021 May 4) 4864, https://doi.org/10.3390/ijms22094864.
[28] Y. Zhao, W. Wei, M.L. Liu, Extracellular vesicles and lupus nephritis - new insights into pathophysiology and clinical implications, J. Autoimmun. 115 (2020 Dec 1) 102540, https://doi.org/10.1016/j.jaut.2020.102540.
[29] M. Horak, J. Novak, J. Bienertova-Vasku, Muscle-specific microRNAs in skeletal muscle development, Dev. Biol. 410 (1) (2016) 1–13, https://doi.org/10.1016/j.ydbio.2015.12.013.
[30] J. Guduric-Fuchs, A. O'Connor, B. Camp, C.L. O'Neill, R.J. Medina, D.A. Simpson, Selective extracellular vesicle-mediated export of an overlapping set of microRNAs from multiple cell types, BMC Genom. 13 (1) (2012), https://doi.org/10.1186/1471-2164-13-357.
[31] J. Cortes-Troncoso, S.I. Jang, P. Perez, J. Hidalgo, T. Ikeuchi, T. Greenwell-Wild, et al., T cell exosome-derived miR-142-3p impairs glandular cell function in Sjögren's syndrome, JCI Insight 5 (9) (2020) 1–14, https://doi.org/10.1172/jci.insight.133497.
[32] S. Sharma, Immunomodulation: a definitive role of microRNA-142, Dev. Comp. Immunol. 77 (2017) 150–156, https://doi.org/10.1016/j.dci.2017.08.001.
[33] J.X. Zhang, W. Yang, J.Z. Wu, C. Zhou, S. Liu, H.B. Shi, et al., MicroRNA-32-5p inhibits epithelial-mesenchymal transition and metastasis in lung adenocarcinoma by targeting SMAD family 3, J. Cancer 12 (8) (2021) 2258–2267, https://doi.org/10.7150/jca.48387.
[34] R.D. Kamdar, B.S. Harrington, E. Attar, S. Korrapati, J. Shetty, Y. Zhao, et al., NF-κB signaling modulates miR-452-5p and miR-335-5p expression to functionally decrease epithelial ovarian cancer progression in tumor-initiating cells, Int. J. Mol. Sci. 24 (9) (2023 Apr 25) 7826, https://doi.org/10.3390/ijms24097826.
[35] M. Tomé, P. López-Romero, C. Albo, J.C. Sepúlveda, B. Fernández-Gutiérrez, A. Dopazo, et al., miR-335 orchestrates cell proliferation, migration and differentiation in human mesenchymal stem cells, Cell Death Differ. 18 (6) (2011 Jun 17) 985–995, https://doi.org/10.1038/cdd.2010.167.
[36] Y. Yu, S. Park, H. Lee, E.J. Kwon, H.R. Park, Y.H. Kim, et al., Exosomal hsa-miR-335-5p and hsa-miR-483-5p are novel biomarkers for rheumatoid arthritis: a development and validation study, Int. Immunopharm. 120 (April) (2023 Jul) 110286, https://doi.org/10.1016/j.intimp.2023.110286.
[37] K. Dopytalska, A. Czaplicka, E. Szymańska, I. Walecka, The essential role of micrornas in inflammatory and autoimmune skin diseases—a review, Int. J. Mol. Sci. 24 (11) (2023 May 23) 9130, https://doi.org/10.3390/ijms24119130.
[38] W. Chen, D. Liu, Q.Z. Li, H. Zhu, The function of ncRNAs in rheumatic diseases, Epigenomics 11 (7) (2019 May) 821–833, https://doi.org/10.2217/epi-2018-0135.
[39] J. Sode, S.B. Krintel, A.L. Carlsen, M.L. Hetland, J.S. Johansen, K. Hørslev-Petersen, et al., Plasma microRNA profiles in patients with early rheumatoid arthritis

responding to adalimumab plus methotrexate vs methotrexate alone: a placebo-controlled clinical trial, J. Rheumatol. 45 (1) (2018 Jan) 53–61, https://doi.org/10.3899/jrheum.170266.
[40] T.L. Suber, L. Casciola-Rosen, A. Rosen, Mechanisms of disease: autoantigens as clues to the pathogenesis of myositis, Nat. Clin. Pract. Rheumatol. 4 (4) (2008) 201–209, https://doi.org/10.1038/ncprheum0760.
[41] A. Letafati, S. Najafi, M. Mottahedi, M. Karimzadeh, A. Shahini, S. Garousi, et al., MicroRNA let-7 and viral infections: focus on mechanisms of action, Cell. Mol. Biol. Lett. 27 (1) (2022), https://doi.org/10.1186/s11658-022-00317-9.
[42] C. Nejad, H.J. Stunden, M.P. Gantier, A guide to miRNAs in inflammation and innate immune responses, FEBS J. 285 (2018) 3695–3716, https://doi.org/10.1111/febs.14482.
[43] S. Roush, F.J. Slack, The let-7 family of microRNAs, Trends Cell Biol. 18 (2008) 505–516, https://doi.org/10.1016/j.tcb.2008.07.007.
[44] V. Salvi, V. Gianello, L. Tiberio, S. Sozzani, D. Bosisio, Cytokine targeting by miRNAs in autoimmune diseases, Front. Immunol. (2019) 10–15, https://doi.org/10.3389/fimmu.2019.00015.
[45] N. Sugito, K. Heishima, Y. Akao, Chemically modified MIR143-3p exhibited anti-cancer effects by impairing the KRAS network in colorectal cancer cells, Mol. Ther. Nucleic Acids 30 (December) (2022 Dec) 49–61, https://doi.org/10.1016/j.omtn.2022.09.001.
[46] Z. Yang, S. Lu, Y. Wang, H. Tang, B. Wang, X. Sun, et al., A novel defined necroptosis-related miRNAs signature for predicting the prognosis of colon cancer, Int. J. Gen. Med. 15 (2022 Jan) 555–565, https://doi.org/10.2147/IJGM.S349624.
[47] S.E. Gomes, D.M. Pereira, C. Roma-Rodrigues, A.R. Fernandes, P.M. Borralho, C.M. P. Rodrigues, Convergence of miR-143 overexpression, oxidative stress and cell death in HCT116 human colon cancer cells, in: A. Ahmad (Ed.), PLoS One 13 (1) (2018 Jan 23) e0191607, https://doi.org/10.1371/journal.pone.0191607.
[48] C.A. Mecoli, T. Igusa, M. Chen, X. Wang, J. Albayda, J.J. Paik, et al., Subsets of idiopathic inflammatory myositis enriched for contemporaneous cancer relative to the general population, Arthritis Rheumatol. 75 (4) (2023 Apr 16) 620–629, https://doi.org/10.1002/art.42311.
[49] K. Patasova, I.E. Lundberg, M. Holmqvist, Genetic influences in cancer-associated myositis, Arthritis Rheumatol. 75 (2) (2023 Feb 20) 153–163, https://doi.org/10.1002/art.42345.
[50] A.A. Aravin, R. Sachidanandam, A. Girard, K. Fejes-Toth, G.J. Hannon, Developmentally regulated piRNA clusters implicate MILI in transposon control, Science 316 (5825) (2007 May 4) 744–747, https://doi.org/10.1126/science.1142612.
[51] K.J. Rayford, A. Cooley, J.T. Rumph, A. Arun, G. Rachakonda, F. Villalta, et al., piRNAs as modulators of disease pathogenesis, Int. J. Mol. Sci. 22 (5) (2021 Feb 27) 2373, https://doi.org/10.3390/ijms22052373.
[52] R. Ren, H. Tan, Z. Huang, Y. Wang, B. Yang, Differential expression and correlation of immunoregulation related piRNA in rheumatoid arthritis, Front. Immunol. 14 (May) (2023 May 30) 1–12, https://doi.org/10.3389/fimmu.2023.1175924.
[53] L. Pleštilová, M. Neidhart, G. Russo, M. Frank-Bertoncelj, C. Ospelt, A. Ciurea, et al., Expression and regulation of PIWIL-proteins and PIWI-interacting RNAs in rheumatoid arthritis, in: D. Heymann (Ed.), PLoS One 11 (2016) e0166920, https://doi.org/10.1371/journal.pone.0166920 eCollection 2016.